2014

A novel magnetorheological elastomer isolator with negative changing stiffness for vibration reduction

Jian Yang
University of Wollongong, jy937@uowmail.edu.au

Shuaishuai Sun
University of Wollongong, ss886@uowmail.edu.au

Haiping Du
University of Wollongong, hdu@uow.edu.au

Weihua Li
University of Wollongong, weihuali@uow.edu.au

Gursel Alici
University of Wollongong, gursel@uow.edu.au

See next page for additional authors

Publication Details

Yang, J., Sun, S. S., Du, H., Li, W. H., Alici, G. & Deng, H. X. (2014). A novel magnetorheological elastomer isolator with negative changing stiffness for vibration reduction. Smart Materials and Structures, 23 (10), 105023-1-105023-11.

A novel magnetorheological elastomer isolator with negative changing stiffness for vibration reduction

Abstract
Magneto-rheological elastomers (MREs) have attracted notable credits in the development of smart isolators and absorbers due to their controllable stiffness and damping properties. For the purpose of mitigating unwanted structural and/or machinery vibrations, the traditional MRE-based isolators have been generally proven effective because the MR effect can increase the stiffness when the magnetic field is strengthened. This study presents a novel MRE isolator that experienced reduced stiffness when the applied current was increased. This innovative work was accomplished by applying a hybrid magnet (electromagnet and permanent magnets) onto a multilayered MRE structure. To characterise this negative changing stiffness concept, a multilayered MRE isolator with a hybrid magnet was first designed, fabricated and then tested to measure its properties. An obvious reduction of the effective stiffness and natural frequency of the proposed MRE isolator occurred when the current was continuously adjusted. This device could also work as a conventional MRE isolator as its effective stiffness and natural frequency also increased when a negative current was applied. Further testing was carried out on a one-degree-of-freedom system to assess how effectively this device could isolate vibration. In this experiment, two cases were considered; in each case, the vibration of the primary system was obviously attenuated under ON-OFF control logic, thus demonstrating the feasibility of this novel design as an alternative adaptive vibration isolator.

Keywords
elastomer, isolator, negative, magnetorheological, changing, novel, stiffness, vibration, reduction

Disciplines
Engineering | Physical Sciences and Mathematics

Publication Details
Yang, J., Sun, S. S., Du, H., Li, W. H., Alici, G. & Deng, H. X. (2014). A novel magnetorheological elastomer isolator with negative changing stiffness for vibration reduction. Smart Materials and Structures, 23 (10), 105023-1-105023-11.

Authors
Jian Yang, Shuaishuai Sun, Haiping Du, Weihua Li, Gursel Alici, and Huaxia Deng

A novel magnetorheological elastomer isolator with negative changing stiffness for vibration reduction

J. Yang[1], S.S. Sun[1], H. Du[2], W.H. Li*[1], G. Alici[1], and H.X. Deng[3]

[1] *School of Mechanical, Material and Mechatronic Engineering, University of Wollongong, New South Wales, 2522, Australia*

[2] *School of Electrical, Computer and Telecommunications Engineering, University of Wollongong, New South Wales, Australia*

[3] *School of Instrument Science and Opto-electronics Engineering, Hefei University of Technology, Hefei, China*

Abstract

Magneto-rheological elastomers (MREs) have attracted notable credits in the development of smart isolators and absorbers due to their controllable stiffness and damping properties. For the purpose of mitigating unwanted structural and/or machinery vibrations, the traditional MRE based isolators have generally proven effective because the MR effect can increase the stiffness when the magnetic field is strengthened. This study presents a novel MRE isolator that its stiffness was reduced when the applied current was increased. This innovative work was accomplished by applying a hybrid magnet (electromagnet and permanent magnets) onto a multilayered MRE structure. To characterise this negative changing stiffness concept, a multilayered MRE isolator with a hybrid magnet was first designed, fabricated, and then tested to measure its properties. An obvious reduction of the effective stiffness and natural frequency of the proposed MRE isolator occurred when the current was continuously adjusted. On the other hand, this device could also work as a conventional MRE isolator as its effective stiffness and natural frequency also increased when a negative current was applied. Further testing was carried out on a 1-degree-of-freedom system to assess how effectively this device isolated vibration. In this experiment, two cases were considered, and in each case vibration of the primary system was obviously attenuated under ON-OFF control logic, thus demonstrating the feasibility of this novel design as an alternative adaptive vibration isolator.

Keywords: MRE isolator, variable stiffness, permanent magnet, control logic, vibration isolation

1. Introduction

As a solution to addressing undesirable vibration, MRE based devices have become a promising choice because the shear modulus of MRE can be controlled rapidly, continuously, and reversibly by an external magnetic field [1-2]. These MRE devices possess a high adaptability because their stiffness can be controlled by external magnetic fields in real time, which, therefore, can suppress vibration by absorption or isolation. In recent years a great deal of exploration on the potential of MRE based absorbers has been done, and the achievements made so far [3-8] have advanced the development and implementation of MRE absorbers quite considerably. Unlike MRE absorbers, using MRE as a variable stiffness element in the development of an adaptive isolator is a relatively new and rarely explored area of research, although studies on isolation systems are ongoing. MRE based isolators tend to attenuate the vibrations of an isolated structure by changing its lateral stiffness in real time, and when a multi-layered MRE is considered, the isolator will satisfy the required vertical load capacity while maintaining horizontal flexibility. For this reason, an adaptive MRE isolator has become a clear advantage over the passive isolation system because the passive isolation cannot adjust its characteristics with respect to the change of the external excitations once it is designed and installed [9-10]. Upon the smart nature, the overarching goal of employing the MRE isolator in an isolation system is to shift the natural frequency of the primary structure as far away as possible from the excitation frequency in time. Therefore, the MRE isolator is superior to the hybrid isolation system (such as viscous liquid damper and friction damper) [11-13] and the smart base isolation system (such as piezoelectric friction damper and magnetorheological (MR damper) [14-15] in that hybrid isolation system and smart base isolation system isolate the disturbance by introducing additional damping into the system which may cause danger or thorny issues [16].

Due to its high efficiency and facility, the development of an MRE based isolator has become a pressing need, which is why a great deal of effort has been expended on investigating and developing a highly adjustable MRE isolator [17-18]. Hwang *et al* [19] conducted a conceptual study on using MRE on a base isolation system for building structures. Usman *et al* [20] numerically evaluated the dynamic performance of a smart isolation system using MRE and validated the feasibility of isolating unwanted vibration using a structure with five degrees of freedom. The results showed that an MRE isolation system outperformed a conventional system by reducing the response of a structure under various seismic excitations. Behrooz *et al* [21] presented the performance of a variable stiffness and damping isolator (VSDI) utilising MRE in a scaled building system. The experimental results showed how VSDIs reduced the acceleration and relative displacement of building floors. A vibration isolation system which used four MRE elements as a tunable spring was reported in [22], and in this study, the proposed MRE isolator successfully suppressed the response of the payload. Li *et al* presented a successful development and experimental evaluation of a smart base isolation utilising MRE in [23].The main contribution of this study is that the MRE isolator used a laminated structure for the traditional base isolator, where multiple layers of thin MRE sheets were bonded onto thin steel plates, which enabled the isolator to maintain high vertical stiffness while simultaneously minimising lateral stiffness. The results of this experiment

showed that the force of the MRE isolator increased up to 45% and the stiffness increased up to 38%; thus demonstrating the potential of the proposed MRE isolator for smart base isolation applications. In order to achieve a larger range of increased stiffness under an applied magnetic field, a further effort has been conducted by Li and his group [24-25], which also tried to find the optimal configuration for a magnetic circuit designed to provide a strong and uniform magnetic field in MRE. A new and highly adjustable MRE isolator was fabricated which increased the force by up to 1579% and the stiffness by up to 1730%. To facilitate further development of the structural control using such an adaptive MRE based isolator, modelling work has been done to simulate its behaviour [26].

Undoubtedly, the development of an MRE isolator has made considerable progress. More importantly, the feasibility and efficiency of an MRE isolator as a potential candidate for a vibration isolation system has been proven. However, its advantages are not confined to the achievements reported. The potential of MRE isolators can be explored even further. With a traditional MRE isolator the focus is on the MR effect such that the force and lateral stiffness can only be increased by the magnetic field; whereas in this study, a new MRE isolator which can achieve 'negative stiffness' has been designed, fabricated, and evaluated. The functionality of 'negative stiffness' was realised by incorporating a hybrid magnetic system (electromagnetic coil and permanent magnets) into the manufacturing process. The significance of including a hybrid magnetic system rests with the new functionality that allows the force and the lateral stiffness of the MRE isolator to be increased and decreased. If a traditional MRE isolator with only an electromagnetic coil is required to achieve 'negative stiffness', the electromagnetic coil must always be on in order to provide a nominal magnetic field to the MRE elements and then the stiffness of the isolator can be increased or decreased by increasing or decreasing the current level, which is costly and dangerous due to the power consumed and the heat produced by the coil. This new design includes permanent magnets that avoid these drawbacks while still providing a safe and energy efficient solution to increasing and decreasing the lateral stiffness of an MRE isolator.

After the introduction, a detailed description of the hybrid magnetic system is provided, and then a new MRE isolator with a hybrid magnetic system is fabricated. In order to characterise the proposed MRE isolator, a series of dynamic tests were carried out in Section 3, including the transmissibility and phase responses which showed that the natural frequency of the MRE isolator can be increased and decreased, and also proved that the lateral stiffness of an MRE isolator can be both above and below a nominal value. In Section 4, vibration isolation experiments were conducted to verify whether the proposed MRE isolator could reduce unwanted vibrations. The conclusions were made in Section 5.

2. Design and Fabrication

2.1 Fabrication of a multilayered MRE structure

The components used to fabricate an MRE include silicone sealant (Selleys Pty. Ltd), silicone oil (Sigma-Aldrich Pty. Ltd), and carbonyl iron particles (C3518, Sigma-Aldrich Pty Ltd). The weight ratio of these three materials was 1.5:1.5:7. After the mixture was stirred thoroughly it was put into a vacuum chamber to eliminate any air bubbles and then placed

into a 1mm thick mold to be cured for 5 days without a magnetic field, after which the isotropic soft MREs were ready for use.

The multilayered MRE structure incorporates a traditional laminated rubber bearing [27-28] that consists of multiple layers of thin MRE sheets and thin steel plates. The inner steel plates give the required vertical load capacity and stiffness, while the MRE sheets offer horizontal flexibility which can be varied instantly under an applied magnetic field. This laminated bearing element consists of 10 layers of 1mm thick by 35mm diameter MRE sheets and 11 layers of 1mm thick by 35mm diameter steel sheets.

2.2 Design of hybrid magnet system

To use this multilayered MRE structure as an adaptive stiffness element, a controllable magnetic system that produces a uniform and powerful magnetic field to energise the low magnetic-conductive MRE materials must first be designed. One of the novel designs that had to be developed for this study was an adjustable hybrid magnet system with permanent magnets and an electromagnetic coil. Although a similar idea can be found in [29] where a hybrid magnetic system was incorporated into an adaptive vibration absorber, the hybrid magnetic system designed and presented by this study differs significantly in its structure and operation compared to [29]. By including permanent magnets, a stable magnetic field could be applied to the laminated MRE and steel structure at all times without any power consumption. Then the electromagnetic coil is responsible for either strengthening or weakening the nominal magnetic field generated by the permanent magnets through adjusting the direction and magnitude of the applied current. The stiffness of the MRE materials was controlled by the superposition of these two magnetic fields. One clear advantage of this design is its ability to increase and decrease the magnitude of the hybrid magnetic field such that the stiffness of the MRE structure can be both increased and decreased such that the natural frequency of the system can be turned to be both above and below the passive natural frequency, which would be a desirable achievement for practical purpose.

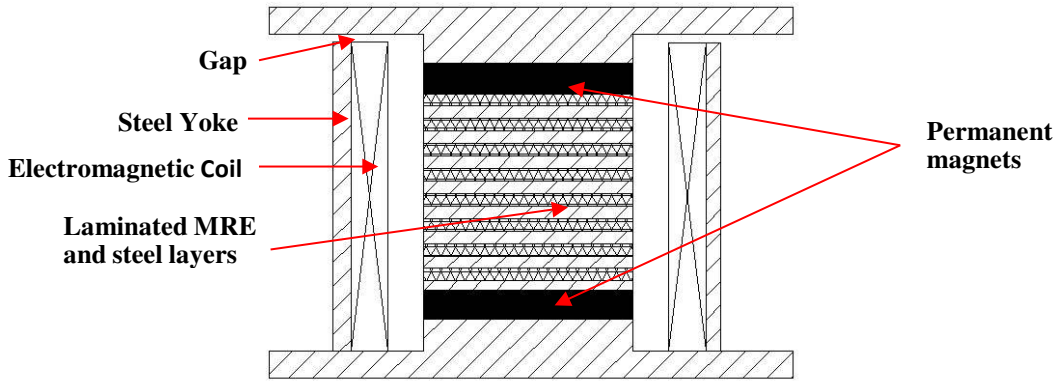

Figure 1. Schematic diagram of the hybrid magnetic system.

Figure 1 shows the assembly of this hybrid magnetic system. To overcome the low magnetic permeability of MRE materials, two steel cylinders were placed at both ends of the laminated structure to increase magnetic conductivity [24] before the laminated structure was placed

between the permanent magnets. The permanent magnets generate a vertical and stable magnetic field perpendicular to the laminated structure, so when this compact structure is placed inside the electromagnetic coil it becomes the magnetic core of the electromagnetic circuit, and because the electromagnetic field inside the solenoid is uniform and vertical, by adjusting the current, the hybrid magnetic system can work in different modes, as shown in Figure 2. The blue closed loop represents the magnetic circuit generated by the permanent magnets, while the yellow loop represents the adjustable magnetic circuit produced by the electromagnetic coil.

In this study, current passing through the coil can generate an electromagnetic field that is opposed to the permanent magnetic field and is defined as a positive current. In this case, as Figure 2a shows, the overall magnitude of the hybrid magnetic field has been reduced. Otherwise, the current that increases the permanent magnetic field is defined as a negative current, as shown in Figure 2b. When a positive current is applied the magnetic field generated by the permanent magnetic field would be reduced by the electromagnetic field, such that the higher the current the more of the magnetic field is reduced, but if the current keeps on increasing, the overall magnitude of the hybrid magnetic field would keep decreasing until it reached zero, after which the hybrid magnetic field would begin to increase in reverse. Correspondingly, the stiffness of the MRE based structure would decrease in the first stage and then increase as the current keeps growing, but when a negative current was applied, the permanent- and electro- magnetic fields would be in the same direction, which means that the superposition of the hybrid magnetic field would be enhanced, and the stiffness of the system would increase until it reached saturation where the negative current keeps increasing.

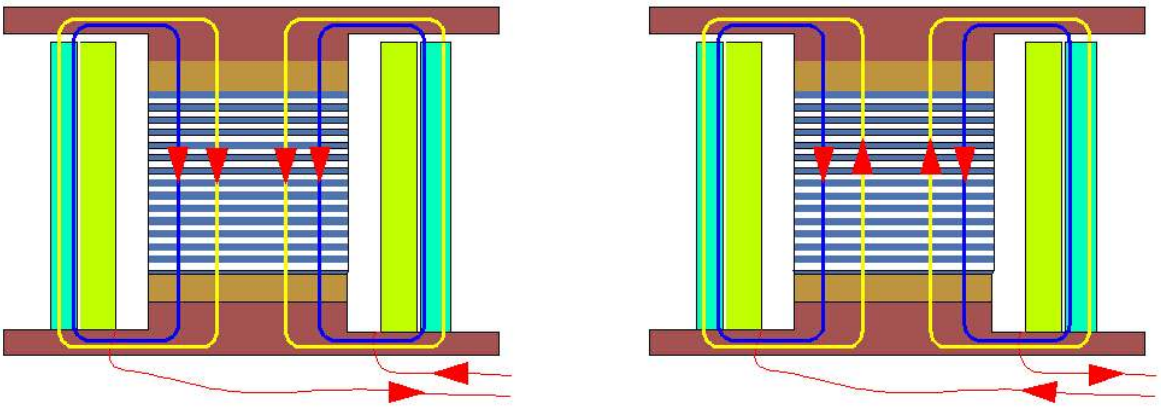

a. Hybrid magnetic field under positive current.

b. Hybrid magnetic field under negative current.

Figure 2. Different working modes for hybrid magnetic system.

2.3 Assembly of MRE based isolator

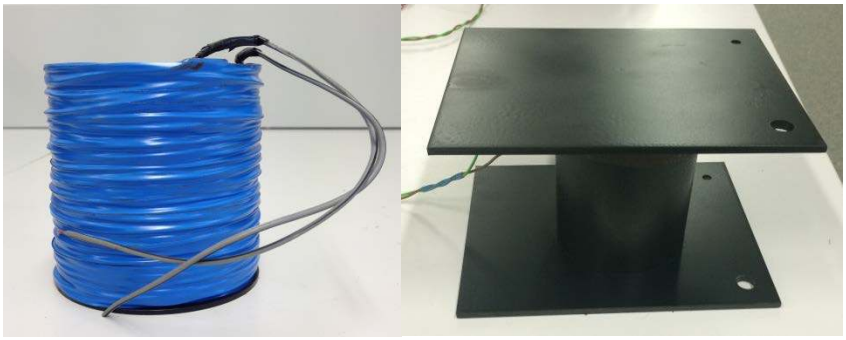

Figure 3. Physical maps for electromagnetic coil and MRE isolator.

Figure 3 shows the physical maps for the electromagnetic coil and the MRE based isolator. The rectangular bottom plate was appropriate for fixing the isolator to the base, through which the disturbance excitation is passed to the whole system. The top steel plate was used to support the weight. Such a novel isolator has inherited the classical laminated structure and incorporated the hybrid magnetic system while being compact enough to be used safely and conveniently, and yet it is strong enough to maintain a high vertical stiffness while simultaneously providing lateral agility. Furthermore, this hybrid magnetic system makes the MRE isolator energy friendly and yet powerful enough to possess a high controllability over its characteristics; attributes that will surely contribute greatly to the engineering world.

3. Characterising the MRE isolator

3.1 Experimental setup

To evaluate and characterise the performance of the MRE base isolator prototype, a series of experimental tests were conducted under various loading conditions. A detailed experimental set up is shown in Figure 4 and a schematic diagram of the experimental set up is shown in Figure 5. The isolator was fixed to the bearing through an aluminum sheet. A base was fabricated to support the bearing in order to avoid any unwanted vibration in the measurement. The isolator was forced to vibrate horizontally by a shaker (VTS, .VC 100-8), which was driven by a signal source from a power amplifier (YE5871), and a laser sensor (MICRO-EPSILON Company) monitored the horizontal movement of the bottom plate. A force sensor (CA-YD-302) was mounted between the top plate of the isolator and the fixed rig to measure the lateral force produced by the isolator. During the test, the top plate and the force sensor remained motionless in order to eliminate any unwanted inertia force in the measurements. A DC power supply (THURLBY-THANDAR, INSTRUMENTS LTD) was used to provide DC current to energise the magnetic coil. The amount and direction of the output current could be adjusted to change the magnitude of the electromagnetic field. The interface connecting the computer and the device (amplifier and signal sensors) was supplied by the Data Acquisition (DAQ) board (LabVIEW PCI-6221, National Instruments Corporation. U.S.A). The LabVIEW program was designed to be the control unit and the display unit where harmonic excitation could be generated and the results displayed and recorded.

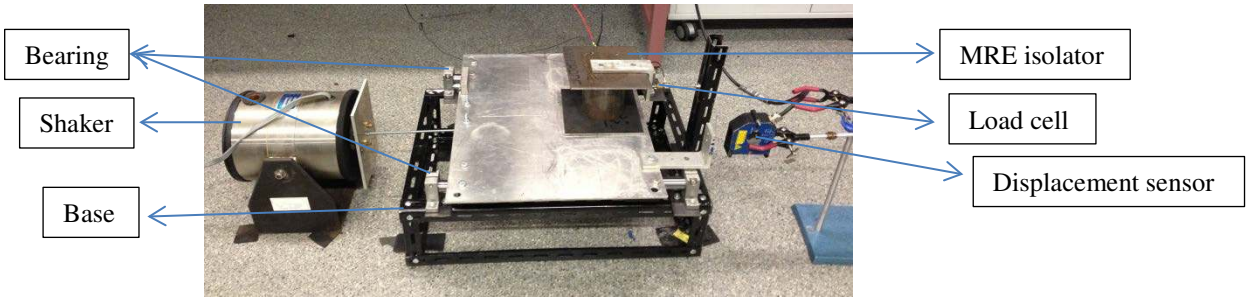

Figure 4. Experimental Setup for testing the MRE isolator.

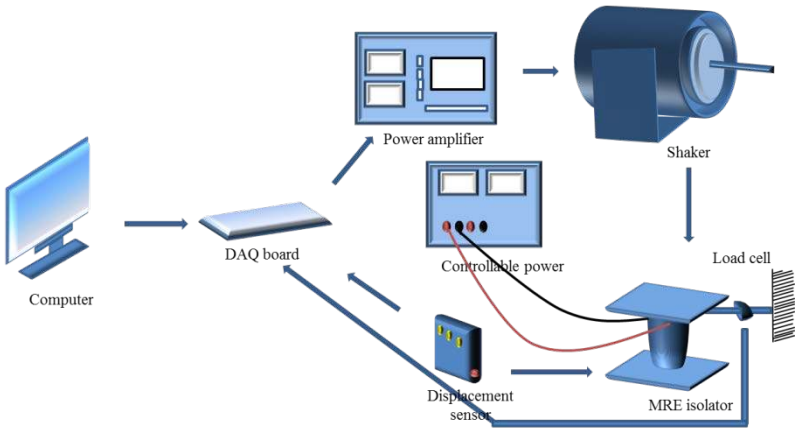

Figure 5. Schematic diagram for the experimental setup.

In the first part of the test various harmonic inputs were used to assess the dynamic properties of the MRE based isolator. A wide range of frequencies, amplitudes, and currents were selected to demonstrate the ability of the isolator to become both 'softer' and 'harder', and both positive (1A, 2A, 3A, and 4A) and negative currents (-1A, -2A, -3A, and -4A) were considered. In each case, the sampling rate for the data acquisition was set to 1000Hz and at least 20 cycles were measured to stabilise the isolator. To further clarify this remarkable progress, the transmissibility and phase of the isolator under different levels of current were also provided. To determine whether this novel design would offer an alternative solution for suppressing vibration, a vibration isolation experiment was conducted as the last part of these experiments.

3.2 Results of Dynamic testing

Figure 6 shows the force-displacement (Figure 6a) and force-velocity (Figure 6b) responses when the MRE isolator was run with a sinusoidal signal of five different amplitudes at a constant frequency (3 Hz) and current (4 A). This series of responses progressed from linear to nonlinear when the loading amplitudes were increased. This can be reasonably explained by the resistance from the rubber matrix and the magnetic force between iron particles that prevented the chain structure in the MRE materials from extending when a larger amplitude was applied. Another obvious finding was the measured force and equivalent damping which was indicated by the enclosed area of the force-displacement loop, and an evident increase in gain with ascending loading amplitudes. However, the lateral stiffness of the isolator,

indicated by the slope of the force-displacement loop, decreased slightly as the amplitude increased.

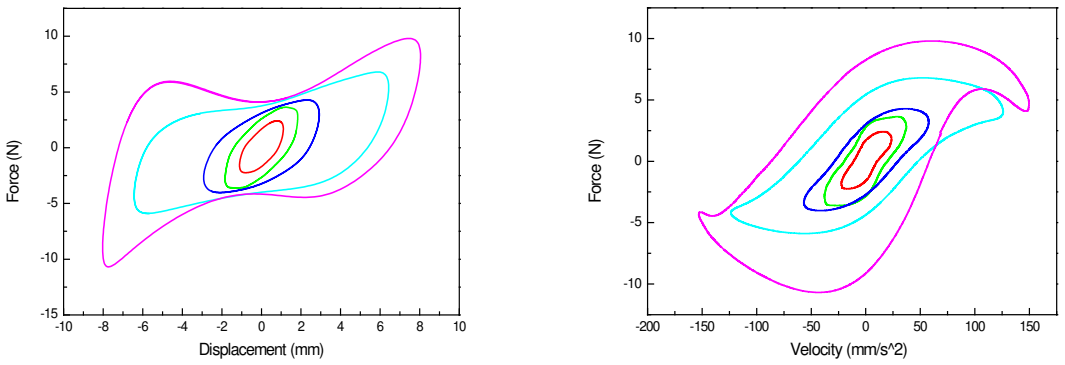

a. Force vs. displacement b. Force vs. velocity

Figure 6. Experimental responses of the MRE isolator under sinusoidal inputs with different amplitudes.

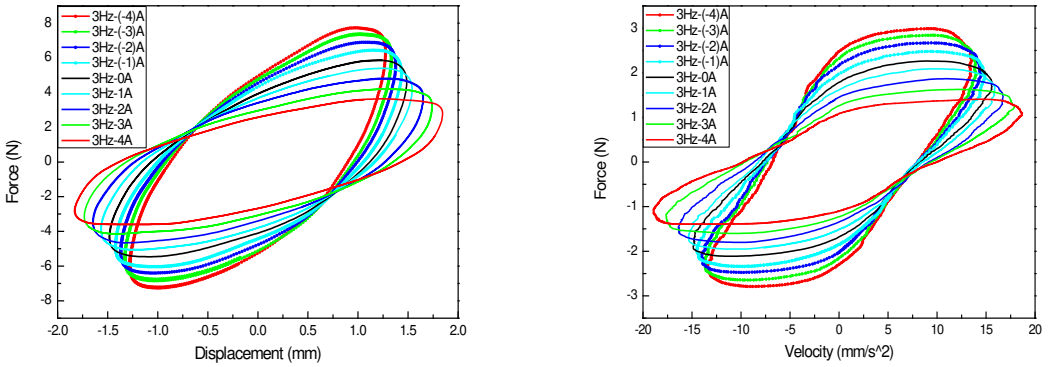

a. Force vs. displacement b. Force vs. velocity

Figure 7. Experimental responses of the MRE isolator under sinusoidal inputs with different currents.

One important highlight of this study was that the hybrid magnetic system enabled the MRE isolator to increase and decrease its lateral stiffness, i.e., the force-displacement and force-velocity performances under different levels of current (different magnetic density) but same frequency and amplitude are presented in Figure 7. As stated earlier, an electromagnetic field opposite to a permanent magnetic field was generated when a positive current was applied; thus the larger the current is, the smaller the superposition of the hybrid magnetic field will be. Contrarily, the hybrid magnetic field will be strengthened. To better describe the special properties the isolator can achieve, it was defined as a benchmark when no current was applied, as highlighted with a black font in Figure 7. But one point must be emphasized: the 'no current' was not equal to its usual passive status because there was a permanent magnetic field working on the system even when no current was applied. Indeed Figure 7 shows that the measured force and lateral stiffness tended to be smaller than the benchmark when a positive current was applied, while the equivalent damping (the enclosed area of the force-displacement loop) decreased as the overall magnitude of the hybrid magnetic system was

reduced. In those cases where a negative current was applied, the measured force, and the lateral stiffness, as well as the equivalent damping, increased as the amount of current grew. The effective stiffness and equivalent damping of each loading case was calculated and is listed in Table 1. The details of the effective stiffness calculation can be found in [23, 30].

Table 1. Effective stiffness of the MRE isolator under various applied currents.

Current (A)	-4	-3	-2	-1	0	1	2	3	4
Effective Stiffness (kN/m)	5.31	5.08	4.62	4.13	3.55	3.15	2.64	2.28	1.88
Equivalent Damping (kN.s/m)	0.2186	0.2028	0.1844	0.1678	0.1500	0.1334	0.1185	0.09896	0.0800

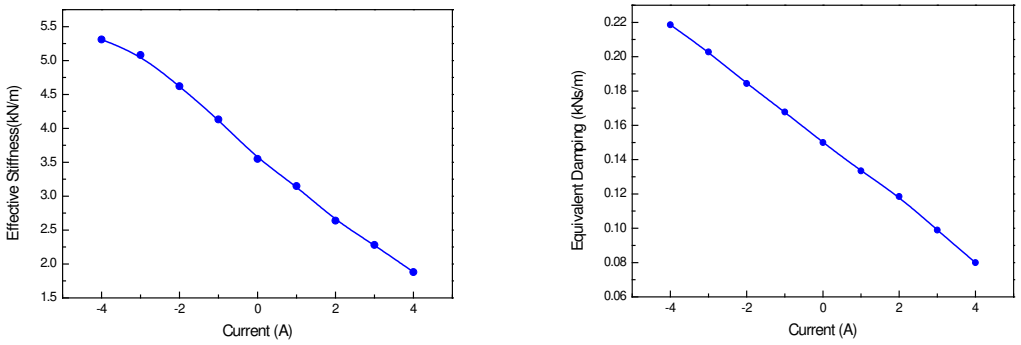

a. Effective stiffness vs. current. b. Equivalent damping vs. current.

Figure 8. Effective stiffness and equivalent damping under various currents.

It can be summarised from the effective stiffness listed in Table 1 that minimum effective stiffness was achieved when the applied current was 4A and the relative change between the minimum and maximum values was 182.4%. Figure 8a shows the relationship between the effective stiffness and the current level, where the effective stiffness was almost a linear function of the applied current in certain areas. Nevertheless, the effective stiffness was not evenly distributed when corresponding to the current, especially when the current was larger. A closer observation reveals that the relative increase of effective stiffness was smaller as the current diverged from zero negatively, which can reasonably be explained as follows. When the current changed to become negative from 0A, the hybrid magnetic field was strengthened as the current kept growing, so initially, the lateral stiffness of the isolator also kept on rising until it eventually reached its saturation point after it increased to a certain value. This explanation applies to Figure 8a where the current was negative and the curve gradually tended to become saturated. For those cases where the current was positive, the superposition of the hybrid magnetic field decreased at first and then increased inversely after it reached zero; therefore there must be a critical current that generates just enough of an electromagnetic field to totally eliminate the permanent magnetic field. Accordingly, the

lateral stiffness of the isolator will decrease until it reaches its minimum and then begin to grow. Unfortunately, this critical point cannot be observed from Figure 8a due to the experimental limitation for a higher current level, but the effective stiffness still decreased linearly in terms of an ascending positive current. As with the effective stiffness, the equivalent damping presented by Figure 8b shows a linear relationship in terms of the current. The calculated equivalent damping can be increased or decreased along with the positive or negative current, which matches well with the observations from Figure 7.

3.3 Transmissibility and Phase responses

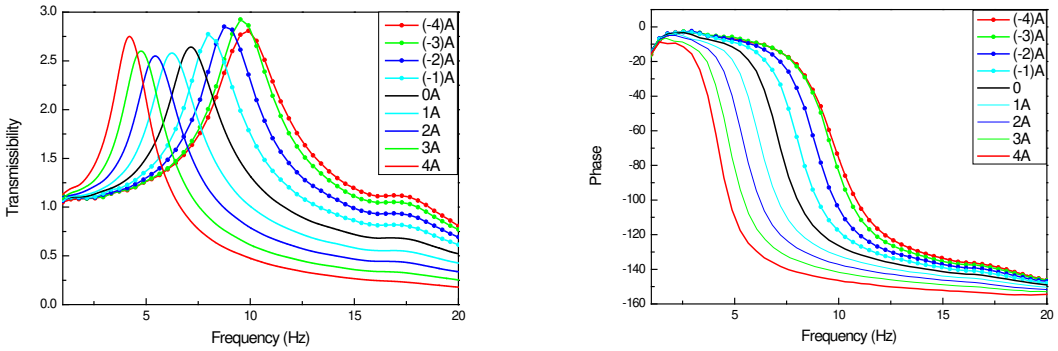

a. Transmissibility vs. frequency. b. Phase vs. frequency

Figure 9. Transmissibility and phase of the MRE isolator under different magnetic field intensity.

Table 2. Natural frequency of the MRE isolator under various applied currents.

Current (A)	-4	-3	-2	-1	0	1	2	3	4
Natural Frequency (Hz)	9.85	9.60	8.89	8.04	7.14	6.23	5.43	4.75	4.20

In this test two accelerometers (CA-YD-106) were installed to measure the lateral acceleration of the top and bottom plates of the isolator respectively. In each case, a sinusoidal excitation with a frequency range sweeping from 1Hz to 20 Hz was used to drive the isolator under various current levels. Figure 9 presents the transmissibility and phase performances of the device under different loading conditions and Table 2 captures the natural frequency in each single case. Here the natural frequency shifted from 9.85Hz to 4.2Hz as the currents changed from -4A to 4A. The relative change in the natural frequency for these two edge cases was about 135%, demonstrating that the natural frequency of this isolation system can be increased and decreased from a nominal value. As the natural frequency of one system is expressed by:

$$f_0 = \frac{1}{2\pi}\sqrt{\frac{k_{eff}}{m}} \tag{1}$$

where f_0, k_{eff}, and m present the natural frequency, effective stiffness, and mass of the system, respectively. The relationship between the natural frequency and the current should

show similarities between the effective stiffness and the current. As expected, Figure 10 shows that the trajectory of the natural frequency-current curve progress was identical to that shown in Figure 8. On one hand the natural frequency changed almost linearly in terms of applied current in some limited areas, but when the current increased or decreased to a larger level negatively or positively, the natural frequency of the isolator kept climbing until it was saturated or it dropped to a minimum before it began to increase again.

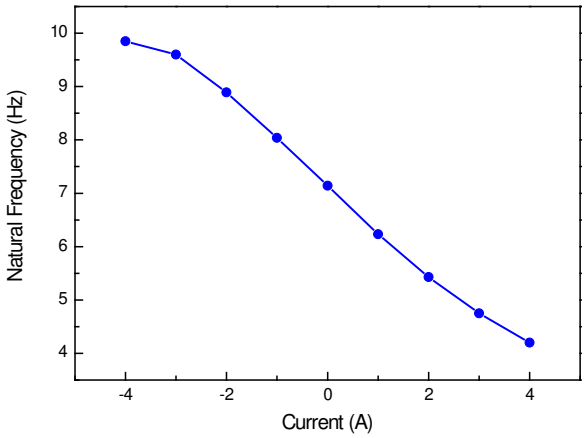

Figure 10. Natural frequency as a function of the current.

4. Vibration isolation experiment

A vibration isolation experiment was conducted to assess the effectiveness of the MRE isolator as an isolation device. As Figure 11 shows, the mass attached to the top plate of the isolator served as the primary system. To determine the feasibility of the device as a vibration isolation system, two testing cases were included in this part. In the first case sinusoidal signals with a constant frequency were used as the means of excitation such that further testing subjected the system to a swept sinusoidal signal. In this testing system, the interface used was a Hilink (ZELTOM) board, as shown in Figure 11. The HILINK platform offers a seamless interface between physical plants and Matlab/Simulink to implement hardware-in-the-loop real-time control systems. It is fully integrated into Matlab/Simulink and has a broad range of inputs and outputs. Through the HILINK board, the displacement signal was input to the computer after being captured by the displacement sensor. After the captured signal was processed by the Simulink block, the block generated a current signal to the HILINK output channel, through which the output signal was sent to the amplifier.

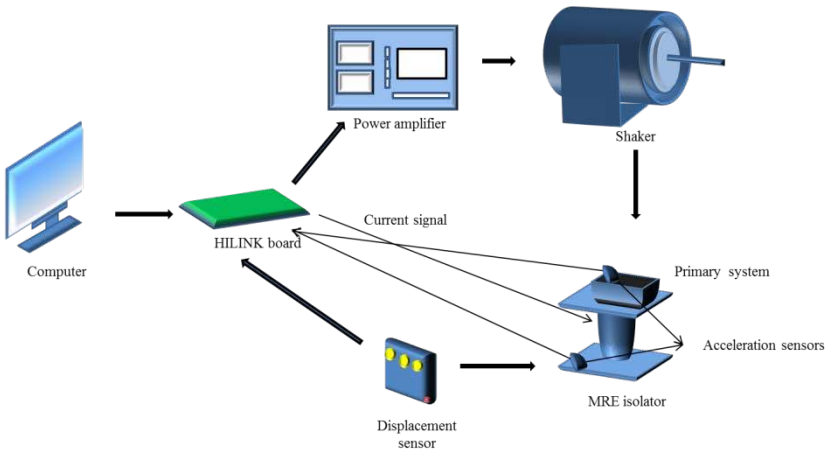

Figure 11. Schematic diagram of the vibration isolation experiment.

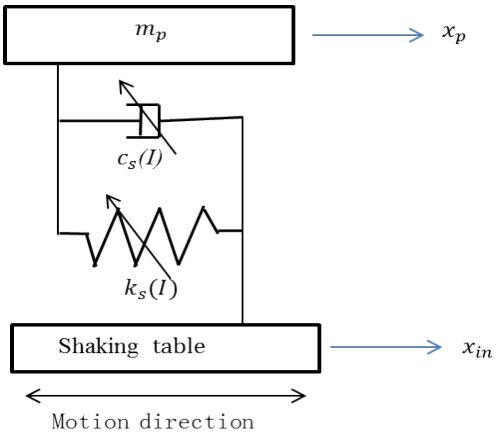

Figure 12. The single-degree-of-freedom system.

The mathematic model of the vibration isolation system can be represented by a single-degree-of–freedom system, as shown in Figure 12. m_p is the mass of the primary system; $c_s(I)$ and $k_s(I)$ represent the controllable damping coefficient and lateral stiffness of the MRE isolator, respectively; x_p and x_{in} are the displacements of the primary system and the driving signal, respectively. The dynamic equation for the system is governed by:

$$m_p\ddot{x}_p + c_s(I)\left(\dot{x}_p - \dot{x}_{in}\right) + k_s(I)\left(x_p - x_{in}\right) = 0 \tag{2}$$

The control algorithm chosen herein, i.e. ON-OFF control, aimed to shift the primary frequency as far away as possible from the frequency of the driving signal. The working logic of the ON-OFF control is such that the lateral stiffness and damping of the isolator will be decreased if the product of the relative displacement and relative velocity of the primary system with respect to the driving excitation is below zero. In other words, a positive current will be chosen if $x_p - x_{in}$ and $\dot{x}_p - \dot{x}_{in}$ are opposite to each other. Otherwise, if the relative displacement and relative velocity are in the same direction, lateral stiffness and damping should be increased. This control logic is concise and simple and yet efficient enough to obtain real time control. The ON-OFF control law is expressed as [31]:

$$I = \begin{cases} 0, & if\,(x_p - x_{in})(\dot{x_p} - \dot{x_{in}}) > 0 \\ I_{MAX}, & if\,(x_p - x_{in})(\dot{x_p} - \dot{x_{in}}) < 0 \end{cases} \quad (3)$$

4.1 Sinusoidal Excitation

In order to obtain the natural frequency of the isolation system with the attached mass, where the input current was zero, the system was first excited by a swept sinusoidal, and the transmissibility is shown in Figure 13. The natural frequency captured was 5.55Hz. Since vibration around a natural frequency is the most severe, three sets of sinusoidal excitation with constant frequency of 5Hz, 5.55Hz, and 7Hz, respectively were used in the first test. To show how effective this vibration isolation was, each testing case was conducted as follows: no control law was applied to the system until the ON-OFF control was turned on; the control law lasted for some time and then it was turned off. This process was done by turning the amplifier, which was connected to the HILINK output channel, on or off.

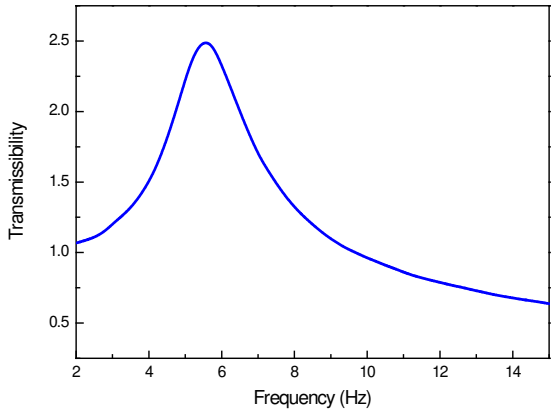

Figure 13. Frequency response of the isolation system.

Figure 14 describes the acceleration measured under different sinusoidal excitations, and in each case, the acceleartion was clearly attenuated during the period when the ON-OFF control logic was working, as marked in Figure 14. The relative changes for each testing were 15%, 23.7%, and 28.6%, respectively, which clearly indicated that the MRE isolator was very efficient in isolating vibration.

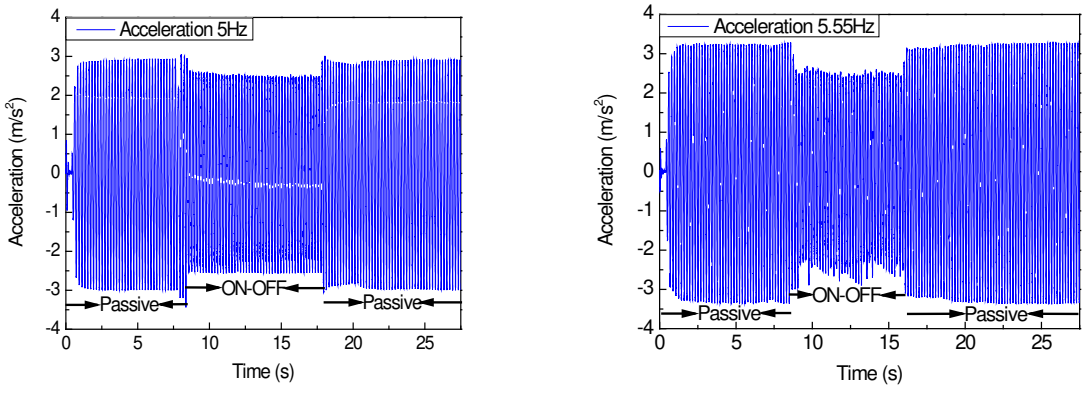

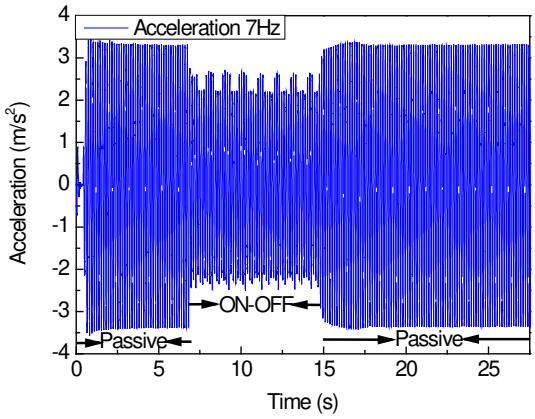

Figure 14. Acceleration responses under different sinusoidal excitations.

4.2 Swept Sinusoidal Excitation

To further evaluate the as-designed vibration isolation system, the response of the primary system under the swept sinusoidal excitation was measured. The working mode without control logic was defined as passive off and the one under ON-OFF control was defined as ON-OFF. A swept sinusoidal covers a frequency band from 2Hz to 15Hz. Figure 15 shows the results for the acceleration of the primary system between passive off and ON-OFF. It was noted that vibration in the primary system was significantly suppressed under the ON-OFF control algorithm, and therefore vibration isolation under the ON-OFF control, as shown by the experimental results, was very effecive.

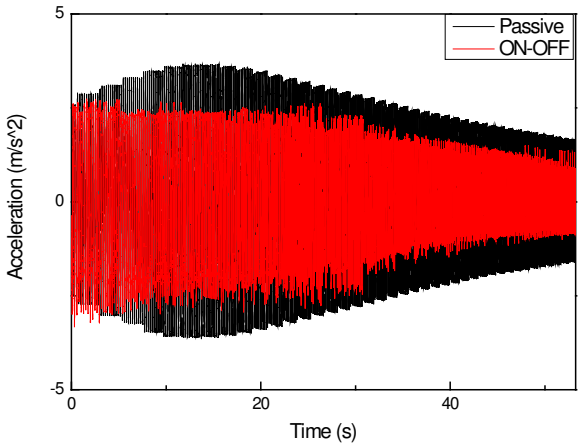

Figure 15. Responses under the swept sinusoidal excitation.

5. Conclusion

A new MRE isolator that includes a hybrid magnetic system was designed and fabricated. This hybrid magnetic system generates a hybrid magnetic field which is the superposition of a permanent magnetic field and an electromagnetic field. The main contribution of this hybrid

magnetic system is that it allows the overall magnitude of a magnetic field to be both increased and decreased, and accordingly, the lateral stiffness of the isolator can be both increased and decreased. To verify the specialty of this isolator, a series of dynamic tests were conducted and the results showed that the effective stiffness was reduced when a positive current was applied, and it grows under a negative current. The transmissibility and phase responses showed that the frequency range of the MRE isolator shifted when the applied current varied from -4A to 4A, thus demonstrating that the natural frequency of the isolation system can be increased and decreased. The isolator was also tested for its ability to avoid unwanted vibrations by subjecting the isolation system to sinusoidal signals with constant frequency and swept sinusoidal signals, respectively. Compared to the passive off case where no current was applied, the acceleration for both cases was obviously reduced under the ON-OFF control logic. The experimental results proved that the proposed MRE isolator is a qualified candidate for vibration isolation applications.

Acknowledgements

This research is supported by an ARC Discovery Grant (No. 140100303), the National Natural Science Foundation of China (Nos. 51205100, & 51328502), and the University of Wollongong and China Scholarship Council joint scholarships (No. 201206450060).

References

[1]. Popp K, Kroger M, Li W, Zhang X, and Kosasih P 2010 MRE Properties under shear and squeeze modes and applications *J. Intell. Mater. Syst. Struct.***21** 1471-1477.

[2]. Li W, Zhou Y and Tian T 2010 Viscoelastic properties of MR elastomers under harmonic loading *Rheol. Acta* **49** 733-740.

[3]. Ni Z, Gong X, Li J, and Chen L 2009 Study on a dynamic stiffness-tuning absorber with squeeze-strain enhanced magnetorheological elastomer *J. Intell. Master. Syst. Struct.* **20** 1195-202.

[4]. Liao G, Gong X, Kang C, and Xuan S 2011 The design of an active-adaptive tuned vibration absorber based on magnetorheological elastomer and its vibration attenuation performance *Smart Mater. Struct.* **20** 075015.

[5]. Hoang N, Zhang N, and Du H 2009 A dynamic absorber with a soft magnetorheological elastomer for powertrain vibration suppression *Smart Mater. Struct.* **18** 1-10.

[6]. Lerner A and Cunefare K 2008 Performance of MRE-based vibration absorber *J. Intell. Mater. Syst. Struct.* **19** 551-63.

[7]. Deng H, Gong X, and Wang L 2006 Development of an adaptive tuned vibration absorber with magnetorheological elastomer *Smart Mater. Struct.* **15** N111.

[8]. Fu J, Zheng X, Yu M, Ju B, and Yang C 2013 A new Magnetorheological elastomer isolator in shear-compression mixed mode *IEEE/ASME International Conf. on Advanced Intelligent Mechatronics* (AIM 2013) July 9-12, Wollongong, Australia, art. No: 6584342, pp.1702-1706.

[9]. Kelly J M 2002 Seismic Isolation Systems for Developing Countries *Earthq. Spectra* **18** 385-406.

[10]. Pan P, Zamfirescu D, Nakashima M, Nakayasu N, and Kashiwa H 2005 Base-isolation design practice in Japan: introduction to the post-Kobe approach *J. Earthq. Eng.***9** 147-171.

[11]. Wongprasert N and Symans M D 2005 Experimental evaluation of adaptive elastomeric base-isolated structures using variable-orifice fluid dampers *J. Struct. Eng.* **131** 867-877.

[12]. Lin P, Roschke P N, and Loh C H 2007b Hybrid base isolation with magneto-rheological damper and fuzzy control *Struct. Contr. Health Monit.* **14** 384-405.
[13]. Kim H S, Roschke P N, Lin P, and Loh C H 2006 Neuro-fuzzy model of hybrid semi-active base isolation system with FPS bearings and an MR damper *Eng. Struct.* **28** 947-958.
[14]. Yoshioka H, Ramallo J C, and Spencer B F Jr 2002 'Smart' base isolation strategies employing magnetorheological dampers *J. Eng. Mech.* **128** 540-551.
[15]. Ramallo J C, Johnson E A, and Spencer B F Jr 2002 'Smart' base isolation systems *J. Eng. Mech.* **128** 1088-1099.
[16]. Mazza F and Vulcano A 2012 Effects of near-fault ground motions on the nonlinear dynamic response of base-isolated R C framed buildings *Earthq. Eng. Struct. Dyn.* **41** 211-32.
[17]. Opie S and Yim W 2009 Design and control of a real-time variable stiffness vibration isolator *IEEE/ASME Int. Conf. Advanced Intelligent Mechatronics (Singapore, July 2009)* pp 380-5.
[18]. Zhu S, Qu L, and Zhou Y 2011 Experimental study of magnetorheological elastomer vibration isolator *Adv. Mater. Res.* **335/336** 1334-9.
[19]. Hwang I H, Lim J H, and Lee J S 2006 A study on base isolation performance of magneto-sensitive rubbers *J. Earthq. Eng. Soc.* **10** 77-84.
[20]. Usman M, Sung S H, Jang D D, Jung H J, and Koo J H 2009 Numerical investigation of smart base isolation system employing MR elastomer *J. Phys. Conf. Ser.* **149** 1-4.
[21]. Behrooz M, Wang X, and Gordaninejad F 2014 Performance of a new magnetorheological elastomer isolation system *Smart Mater. Struct.* **23** 045014.
[22]. Liao G, Gong X, Xuan S, Kang C, and Zong L 2012 Development of a Real-time Tunable Stiffness and Damping Vibration Isolator Based on Magnetorheological Elastomer *J. Intell. Mater. Syst. Struct.* **23** 25-33.
[23]. Li Y, Li J, Li W, and Samali B 2013 Development and characterization of a magnetorheological elastomer based adaptive seismic isolator *Smart Mater. Struct.* **22** 035005.
[24]. Li Y, Li J, Tian T, and Li W 2013 A highly adjustable magnetorheological elastomer base isolator for applications of real-time adaptive control *Smart Mater. Struct.* **22** 095020.
[25]. Li J, Li Y, Li W, and Samali B 2013 Development of adaptive seismic isolators for ultimate seismic protection of civil structures *Proc. SPIE on Sensors and Smart Structures Technologies for Civil, Mechanical, and Aerospace Systems*, Vol. 8692, Art. No. 86920H (12 pages).
[26]. Yang J, Du H, Li W, Li Y, Li J, Sun S, and Deng H 2013 Experimental study and modeling of a novel magnetorheological elastomer isolator *Smart Mater. Struct.* **22** 117001.
[27]. Ronbinson W H 1982 Lead-Rubber hysteretic bearings suitable for protecting structures during earthquakes *Earthq. Eng. Struct. Dyn.* **10** 593-604.
[28]. Fuller K N G, Gough J, Pond T J, and Ahmadi H R 1997 High damping natural rubber seismic isolators *J. Struct. Contr.* **4** 19-40.
[29]. Sinko R, Karnes M, Koo J, Kim Y, and Kim K 2012 Design and test of an adaptive vibration absorber based on magnetorheological elastomers and a hybrid electromagnet *J. Intell. Mater. Syst. Struct.* **24** 803-812.
[30]. Li W, Yao G, Chen G, Yeo S, and Yap F 2000 Testing and steady state modeling of a linear MR damper under sinusoidal loading *Smart Mater. Struct.* **9** 95-102.
[31]. Yang J, Kim J, and Agrawal A 2000 Resetting semi-active stiffness damper for seismic response control *J. Struct. Eng. ASCE* **126** 1427-1433.